Single Giant Unilamellar Vesicle Method Reveals Effect of Antimicrobial Peptide Magainin 2 on Membrane Permeability†

Yukihiro Tamba‡ and Masahito Yamazaki*,‡,§

Materials Science, Graduate School of Science and Engineering, and Department of Physics, Faculty of Science, Shizuoka University, Shizuoka 422-8529, Japan

Received August 24, 2005; Revised Manuscript Received October 17, 2005

ABSTRACT: It is thought that magainin 2, an antimicrobial peptide, acts by binding to lipid membranes. Recent studies using a suspension of large unilamellar vesicles (LUVs) indicate that magainin 2 causes gradual leakage from LUVs containing negatively charged lipids. However, the details of the characteristics of the membrane permeability and the mechanism of pore formation remain unclear. In this report, we investigated the interaction of magainin 2 with single giant unilamellar vesicles (GUVs) composed of a dioleoylphosphatidylcholine and dioleoylphosphatidylglycerol mixture (50% DOPG/50% DOPC GUVs) containing the fluorescent dye, calcein, by phase contrast, fluorescence microscopy using the single GUV method. Low concentrations (3−10 μM) of magainin 2 caused the rapid leakage of calcein from single GUVs but did not disrupt the liposomes or change the membrane structure, showing directly that magainin 2 forms membrane pores through which calcein leaked. The rapid leakage of calcein from a GUV started stochastically, and once it began, the complete leakage occurred rapidly (6−60 s). The fraction of completely leaked GUV, P_L, increased with time and also with an increase in magainin 2 concentration. Shape changes in these GUVs occurred prior to the pore formation and also at lower concentrations of magainin 2, which could not induce the pore formation. Their analysis indicates that binding of magainin 2 to the external monolayer of the GUV increases its membrane area, thereby raising its surface pressure. The addition of lysophosphatidylcholine into the external monolayer of GUVs increased P_L. On the basis of these results, we propose the two-state transition model for the pore formation.

Antimicrobial peptides with bactericidal and fungicidal activity have been found and isolated from a wide variety of organisms, including amphibians, invertebrates, plants, and mammals (*1*, *2*). The target of these peptides is thought to be the lipid membrane region of the bacterial and fungal biomembranes, but the mechanism of the bactericidal activity is controversial, and the details of the interaction between antimicrobial peptides and lipid membranes remain unclear.

Among these antimicrobial peptides, magainin 2, which was at first isolated from the African clawed frog *Xenopus laevis* (*3*, *4*), has been extensively investigated. Magainin 2 forms an α-helix in the lipid membrane interface parallel to the membrane surface (*5*, *6*). Studies with the fluorescent probe, calcein, show that interaction of magainin 2 causes leakage from large unilamellar vesicles (LUVs)[1] containing negatively charged lipids (*7*, *8*). Extensive investigations suggest that this occurs through a pore formed by insertion of several magainin 2 molecules into the lipid membrane (*9*, *10*). However, the characteristics of the pore and the mechanism of pore formation are not currently clear.

Recently, giant liposomes or giant unilamellar vesicles (GUVs) of lipid membranes with diameters greater than 10 μm have been used for investigations of the physical and biological properties of vesicle membranes such as elasticity and shape change (e.g., refs *11*−*16*). The shape of a single GUV and its physical properties in water can be measured in real time. Therefore, GUVs have a great advantage over smaller liposomes such as LUVs and small unilamellar vesicles (SUVs) in investigating the physical properties and structural changes of liposomes. So far, almost all studies of liposomes have been carried out on a suspension of many small liposomes such as LUVs and SUVs using light scattering, fluorescence spectroscopy, electron spin resonance, and X-ray scattering. In these studies, the average values of the physical parameters of liposomes have been obtained from large numbers of liposomes, and thereby much information has been lost (e.g., refs *7*, *8*, *10*, *17*, *18*). In

† This work was supported in part by a Grant-in-Aid for Scientific Research (B) from the Ministry of Education, Science, and Culture (Japan) to M.Y. Most of the content of this work was described in the Ph.D. Thesis of Y.T. (June 2005).

* Correspondence should be addressed to this author at the Department of Physics, Faculty of Science, Shizuoka University. Tel/Fax: 81-54-238-4741. E-mail: spmyama@ipc.shizuoka.ac.jp.

‡ Materials Science, Graduate School of Science and Engineering, Shizuoka University.

§ Department of Physics, Faculty of Science, Shizuoka University.

[1] Abbreviations: GUV, giant unilamellar vesicle; P_L, the fraction of completely leaked GUV at any given time (shortly the fraction of leaked GUV); P_{intact}, the fraction of intact GUV at any given time; P state, pore state; B_{ex} state, binding state in the external monolayer; B_{in} state, binding state in the internal monolayer; P/L, peptide-to-lipid molar ratio; DOPG, 1,2-dioleoyl-*sn*-glycero-3-phospho-*rac*-1-glycerol; DOPC, 1,2-dioleoyl-*sn*-glycero-3-phosphocholine; LUV, large unilamellar vesicle; lyso-PC, lysophosphatidylcholine; PIPES, piperazine-1,4-bis(2-ethanesulfonic acid); EGTA, ethylene glycol bis(β-aminoethyl ether)-*N*,*N*,*N*′,*N*′-tetraacetic acid.

10.1021/bi051684w CCC: $30.25
Published on Web 11/11/2005

contrast, studies of single GUVs provide information on the structure and physical properties of single GUVs as a function of time and spatial coordinates (the single GUV method) (*19*). It is expected that the single GUV method will provide a great deal of new information on the structure and function of biomembranes and lipid membranes which cannot be obtained by the studies on the suspension of LUVs and SUVs (*19*). For example, the single GUV method has been successfully used to study membrane fusion and vesicle fission (*20*, *21*).

In this report, we investigated the interaction of magainin 2 with lipid membranes using the single GUV method. As described above, all previous experiments on the interaction of magainin 2 with liposomes were carried out using LUVs and SUVs. In particular, the leakage of internal contents from liposomes induced by magainin 2 was measured using a suspension of many LUVs, i.e., an ensemble of LUVs (*7*, *8*, *10*). We predicted that we would gain new information on the interaction of magainin 2 with lipid membranes by the single GUV method. For this purpose, we used GUVs of lipid membranes of dioleoylphosphatidylcholine (DOPC) and a negatively charged dioleoylphosphatidylglycerol (DOPG) mixture (i.e., DOPG/DOPC GUVs). Low concentrations (3−10 μM) of magainin 2 induced a rapid leakage of a fluorescent probe, calcein, from the inside of single DOPG/DOPC GUVs without disruption of liposomes or changes in their membrane structure. These results indicate that magainin 2 formed a pore (or pores) in the membrane through which calcein leaked. We further analyzed the characteristics of the magainin 2-induced leakage of calcein from single GUVs and compared it with that from the suspension of LUVs. Shape changes in these GUVs occurred prior to the pore formation and also at lower concentrations of magainin 2, which could not induce the pore formation. The analysis of the magainin 2-induced shape changes shows that binding of magainin 2 to the external monolayer of the GUV increases its membrane area, inducing an increase in its surface pressure. On the basis of these results, we discuss the character of the pore in the membrane and the mechanism of the pore formation by magainin 2.

EXPERIMENTAL PROCEDURES

Materials and Peptide Synthesis. DOPC and DOPG were purchased from Avanti Polar Lipids Inc. (Alabaster, AL). Calcein was purchased from Dojindo Laboratory (Kumamoto, Japan). Bovine serum albumin (BSA) was purchased from Wako Pure Chemical Industry Ltd. (Japan). Peptides were synthesized by the FastMoc method using a 433A peptide synthesizer (PE Applied Biosystems, Foster City, CA). The sequence of magainin 2 (23-mer) is GIGKFLHSAKKFGKAFVGEIMNS, and it has an amide-blocked C terminus. The methods for purification and identification of peptides were described in our previous papers (*16*, *22*). The purified peptides were analyzed by ion spray ionization mass spectrometry using a single quadrupole mass spectrometer (API 150EX, PE SCIEX; PE Applied Biosystems, Foster City, CA). The measured mass of magainin 2 was 2465 ± 1 Da, which corresponds to the molecular mass calculated from their amino acid composition.

Formation and Microscopic Observation of GUVs. GUVs were prepared in buffer by the natural swelling of a dry lipid film at 37 °C as follows (*15*, *21*). One hundred microliters of 1 mM phospholipid mixtures (e.g., DOPG and DOPC) in chloroform was placed in a glass vial (5 mL) and dried under a stream of N_2 gas to produce a thin, homogeneous lipid film. The solvent was completely removed by placing the bottle containing the dry lipid film in a vacuum desiccator connected to a rotary vacuum pump for more than 12 h. Next, 10 μL of water was added into this glass vial, and the mixture was incubated at 45 °C for 10 min (prehydration). The hydrated lipid film was then incubated with 2 mL of buffer A (10 mM PIPES, pH 7.0, 150 mM NaCl, and 1 mM EGTA) containing 0.1 M sucrose or 2 mL of 1 mM calcein in buffer A containing 0.1 M sucrose for 2−3 h at 37 °C. Untrapped calcein was removed as described in our previous report (*23*). The GUV suspension was centrifuged at 14000*g* for 10 min at 20 °C to remove multilamellar vesicles (MLVs). The supernatant was collected and passed through a Sephadex G-75 column with buffer A containing 0.1 M glucose, and the fractions containing GUVs were collected.

A 10 μL aliquot of the GUV solution (containing 0.1 M sucrose solution; internal solution) was diluted into 290 μL of 0.1 M glucose in buffer A (external solution) and then transferred into a handmade microchamber (*15*, *16*). A slide glass was coated with 0.1% (w/v) BSA in buffer A containing 0.1 M glucose. We observed GUVs using an inverted fluorescence phase contrast microscope (IX-70; Olympus, Tokyo, Japan) at 20 ± 2 °C. Phase contrast images and fluorescence images of GUVs were recorded using a CCD camera (DXC-108; Sony, Tokyo, Japan) with a video recorder (*20*, *23*). The fluorescence intensity inside of GUVs was determined using Image J (version 1.33u; National Institutes of Health, Bethesda, MD), and the average intensity per GUV was estimated. As GUVs, we selected vesicles whose membranes had a low contrast and a high undulation motion. Various concentrations of magainin 2 or lyso-PC in buffer A containing 0.1 M glucose were introduced slowly in the vicinity of a GUV through a 20 μm diameter glass micropipet positioned by a micromanipulator. The details of this method are described in our previous reports (*15*, *16*, *21*, *23*).

Formation of LUVs and Interaction of Magainin 2 with DOPG/DOPC LUVs. LUVs of DOPG/DOPC were prepared by the extrusion method using 200 nm pore membranes (*23*). The appropriate amounts of lipids in chloroform were mixed and dried under a stream of N_2 gas, after which the solvent was completely removed by placing the sample in a vacuum desiccator connected to a rotary vacuum pump for more than 12 h. To prepare MLVs, 1 mL of 70 mM calcein in water (pH 7.0; adjusted with NaOH) was added to the dry lipid film, and the suspension was vortexed several times for approximately 30 s at room temperature. Next, the suspension of MLVs was subjected to five cycles of freezing in liquid N_2 for 2 min, followed by warming to room temperature for 20 min (freeze−thawing). The resulting solution was extruded through a 200 nm pore membrane using a LF-1 LiposoFast apparatus (Avestin, Ottawa, Canada) until the solution became transparent. To remove the untrapped calcein, the LUV suspension was passed through a Sephadex G-75 column equilibrated in buffer A. A Hitachi F3000 spectrofluorometer was used for fluorescence measurements. Fluorescence intensities of samples were measured at room temperature. The excitation wavelength was 490 nm, and

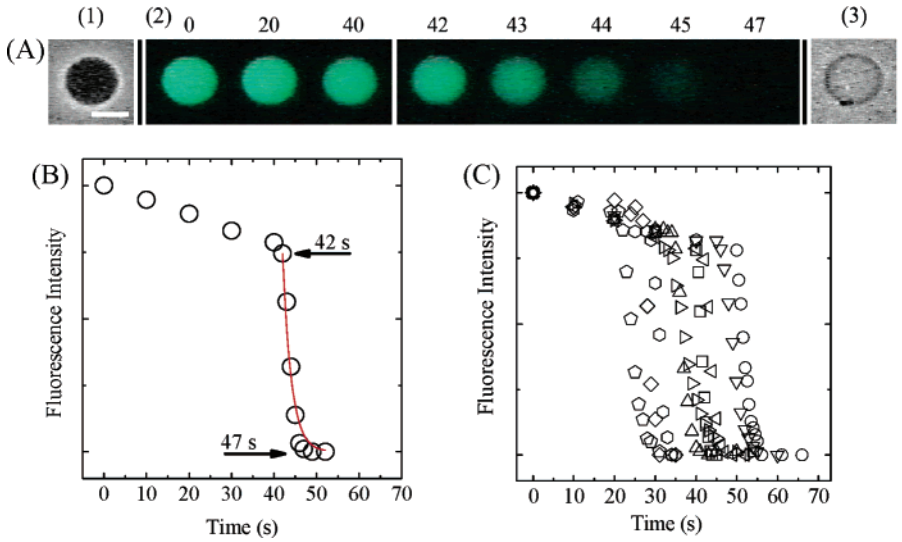

FIGURE 1: Leakage of calcein from single 50% DOPG/DOPC GUVs induced by 7 μM magainin 2. (A) Fluorescence images (2) show that the calcein concentration inside the GUV progressively decreased after the addition of magainin 2. The numbers above each image show the time after the addition. Also shown are phase contrast images of the GUV at 0 s (1) and at 47 s (3). The bar corresponds to 10 μm. (B) Time course of the change of the fluorescence intensity of the GUV shown in (A). A red solid line represents the best fitted curve of eq 7 ($k_{leak} = 0.49\ s^{-1}$; $t_{tr} = 42$ s). (C) Other examples of change in the fluorescence intensity of the GUV with time under the same condition.

the emission wavelength was 520 nm. The excitation and emission band-passes were 1.5 nm. The concentration of total phospholipids in the samples for fluorescence measurements was 42 μM, as determined by the Bartlett method. The fluorescence intensity of the DOPG/DOPC LUV suspension in the absence of magainin 2 and that in the presence of 0.6% (v/v) Triton X-100 were taken as 0% and 100% leakage, respectively.

RESULTS AND DISCUSSION

Induction of Calcein Leakage from DOPG/DOPC (50:50 mol %) GUV (50% DOPG/DOPC) by Magainin 2. We first examined the effect of introducing 7 μM magainin 2 (in buffer A containing 0.1 M glucose at 20 ± 2 °C) in the vicinity of a 50% DOPG/DOPC GUV containing 1 mM calcein. The magainin 2 solution was introduced through a micropipet controlled by a micromanipulator. Before the addition, the GUV had a high contrast in a phase contrast microscopic image [Figure 1A (1)] due to the difference in concentrations of sucrose and glucose between the inside and the outside of the GUV [i.e., 0.1 M sucrose (inside the GUV) and 0.1 M glucose (outside the GUV)]. A fluorescence microscopic image of the same GUV [Figure 1A (2)] shows that there is a high concentration of calcein inside the GUV at this time. During the introduction of the 7 μM solution of magainin 2, there was a gradual reduction in the fluorescence intensity inside the GUV over the first 40 s, after which (42−47 s) the fluorescence intensity decreased rapidly (Figure 1B). After 47 s, fluorescence was not detected inside the GUV, but a phase contrast image of the same GUV [Figure 1A (3)] shows that the GUV was not broken and still existed. We can reasonably consider that the gradual decrease in the fluorescence intensity was due to the photobleaching of calcein, as discussed later. These results clearly show that the leakage of calcein from the inside to the outside of the GUV did not occur as a result of the disruption of the GUV, although this was observed in the interaction of detergents such as Triton X-100 with GUVs (*23*). Figure 1A also shows that, during the leakage of calcein, GUVs did not associate each other and the shape of the GUV did not change (i.e., it was always spherical). This indicates that the leakage of calcein did not occur as a result of instability of the membrane structure due to large deformation of the associated vesicles as has been reported in the interaction of poly(ethylene glycol) with vesicles (*18*). Thereby, we can reasonably consider that calcein leaked from the GUV because of the formation of a pore (or pores) in the membrane by magainin 2. These results, therefore, provide direct evidence for the pore formation in the membrane by magainin 2 as proposed by Matsuzaki and colleagues on the basis of studies of LUVs (*7*, *10*). Comparison of the phase contrast images in Figures 1A (1) and 1A (3) also shows that there was a substantial loss in the contrast of the GUV, indicating that, during the leakage of the calcein, sucrose and glucose passed through the membrane, apparently through the same pore that allowed the calcein leakage. When other 50% DOPG/DOPC GUVs were treated with 7 μM magainin 2 by the same method described above, there was a similar complete leakage of calcein and sucrose in all of the GUVs (Figure 1C); at first, the fluorescence intensity decreased gradually, and at $t = t_{tr}$ the rapid decrease in the fluorescence intensity began to occur. Once the fluorescence intensity started to decrease rapidly, it quickly reached zero within 5.6 ± 0.8 s (Figure 1C), which was determined by the duration between t_{tr} and the time when the fluorescence intensity, $I(t)$, reached 10% of $I(t_{tr})$. This result indicates that once the leakage of calcein started, all of the calcein molecules leaked quickly from the GUVs within 5.6 ± 0.8 s.

We next investigated the effect of 4 μM magainin 2 in the same system. A phase contrast microscopic image prior to the addition of magainin 2 [Figure 2A (1)] showed high contrast, and a fluorescence microscopic image [Figure 2A (2)] revealed a high concentration of calcein inside the GUV. During the addition of 4 μM magainin 2, the fluorescence intensity inside the GUV gradually decreased for the first 135 s, after which there was a rapid decrease between 135 and 170 s [Figure 2B (○)]. After 200 s, there was no fluorescence intensity inside the GUV, although the phase

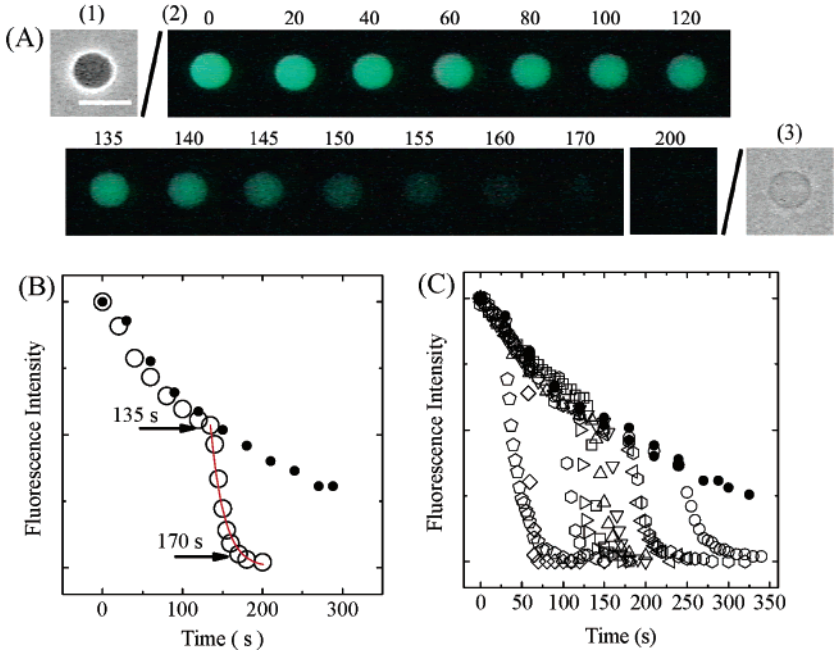

FIGURE 2: Leakage of calcein from single 50% DOPG/DOPC GUVs induced by 4 μM magainin 2. (A) Fluorescence images (2) show that the calcein concentration inside the GUV progressively decreased after the addition of magainin 2. The numbers above each image show the time after the addition. Also shown are phase contrast images of the GUV at 0 s (1) and at 200 s (3). The bar corresponds to 20 μm. (B) Time course of the change of the fluorescence intensity of the GUV shown in (A). A red solid line represents the best fitted curve of eq 7 ($k_{leak} = 0.059$ s^{-1}; $t_{tr} = 135$ s). (C) Other examples of change in the fluorescence intensity of the GUV with time under the same condition.

contrast image [Figure 2A (3)] showed that the GUV was not broken. In contrast, in some GUVs under the same condition, there was only a continual gradual decrease in the fluorescence intensity during the addition of 4 μM magainin 2 (Figure 2B (●)). When we observed single GUVs without the introduction of magainin 2 as a control experiment, we observed only this gradual type of decrease in the fluorescence intensity with the same time dependence. Thereby, we can reasonably consider that this gradual decrease in the fluorescence intensity was due to the photobleaching of calcein. The phase contrast image of the GUV [Figure 2A (3)] shows a large decrease in the contrast as in Figure 2A (1), indicating that, during the leakage of the calcein, sucrose and glucose passed through the pore from which calcein leaked. As the result of the interaction of 7 μM magainin 2 with the GUVs (Figure 1), these results of the effect of 4 μM magainin 2 clearly show that the leakage of calcein and sucrose from the GUV occurred through the pore formed by magainin 2. The rate of the decrease in the phase contrast was rapid compared with that of the decrease in the fluorescence intensity, judging from the result that the fluorescence intensity of the GUV was sufficiently high when the phase contrast between the inside and the outside of the GUV disappeared completely. It indicates that the leakage of sucrose through the pore was faster than that of calcein.

When other 50% DOPG/DOPC GUVs were treated with 4 μM magainin 2 by the same method described above, we found a similar rapid complete leakage of calcein from the GUVs within 5 min in 11 of 16 GUVs. Thus, the probability that a GUV did not contain calcein at 5 min under the same conditions was 0.69. Figure 2C shows the changes in fluorescence intensity of several GUVs under the same conditions as in Figure 2B. After some lag time, the rapid decrease in the fluorescence intensity started stochastically. We can consider that the binding of magainin 2 to a GUV reached equilibrium less than approximately 30 s after its introduction through the micropipet, judging from the result of Figure 1C (see The Two-State Transition Model of the Pore Formation Induced by Magainin 2 for details). Thereby, this result suggests that the pore formation by magainin 2 occurred stochastically.

Characteristics of the Leakage of Calcein from DOPG/DOPC GUV Induced by Magainin 2. The results of Figures 1 and 2 clearly show that the leakage of calcein from the GUV occurred through the pore formed by magainin 2 in the membrane of the GUV and was not mediated by disruption of the vesicle structure. Very recently, Ambroggio et al. reported that β-amyloid peptide and antimicrobial peptides such as maculatin induced the leakage of the fluorescent probe (such as Alexa maleimide) from GUVs, although its quantitative analysis was not undertaken (*24*, *25*). Their results support our conclusion described above.

Here we analyze the magainin 2-induced leakage of calcein from the GUVs quantitatively. As shown in Figures 1C and 2C, the onset of leakage from the GUV due to the pore formation was stochastic. In the case of 50% DOPG/DOPC GUVs, at ≥ 7 μM magainin 2, the complete leakage of calcein from the GUV occurred in all the examined GUVs within 5 min after the introduction of magainin 2. At lower concentrations (3−5 μM), on the other hand, magainin 2 induced the complete leakage of calcein in only some of the examined GUVs within 5 min, but in other GUVs no leakage occurred. At very low concentrations (1−2 μM), we did not observe the rapid decrease in the fluorescence intensity, and thereby, no leakage of calcein was induced by magainin 2. These results indicate that, in the estimation of the leakage of the internal contents of a single liposome, the probability, $P_L(t)$, that a liposome (in this case, a GUV) does not contain

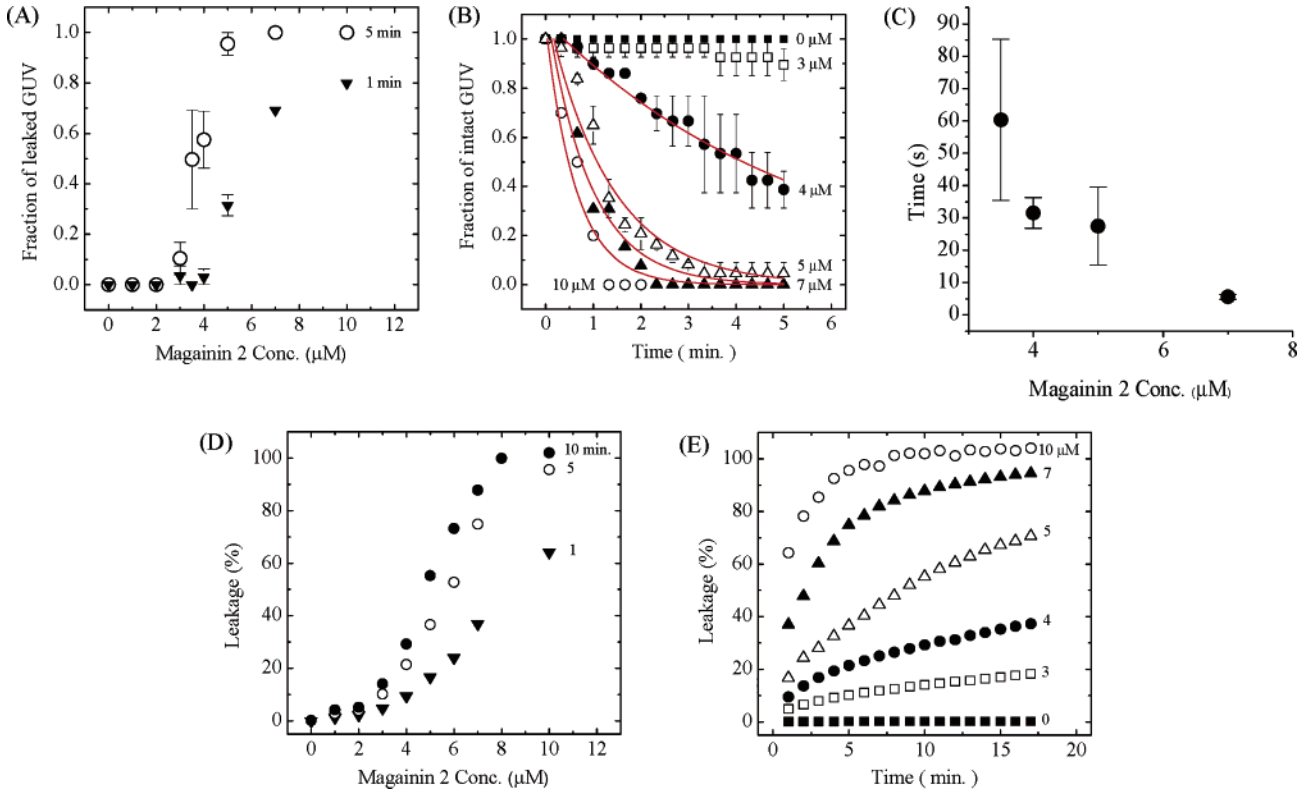

FIGURE 3: (A) Dose−response of magainin 2 for the fraction of completely leaked GUV, $P_L(t)$, among all the 50% DOPG/DOPC GUVs at $t = 5$ min (○) and $t = 1$ min (▼) after the addition of magainin 2. (B) Time course of the fraction of intact GUV, $P_{intact}(t)$, after the addition of various concentrations of magainin 2: (■) 0 μM, (□) 3 μM, (●) 4 μM, (△) 5 μM, (▲) 7 μM, and (○) 10 μM. Red solid lines represent the best fitted curves of eq 6. (C) The time required to leak 90% calcein molecules from single 50% DOPG/DOPC GUVs in the presence of various magainin 2 concentrations. It was determined by the duration between t_{tr} and the time when the fluorescence intensity, $I(t)$, reached 10% of $I(t_{tr})$. (D) Dose−response of magainin 2-induced leakage from a suspension of 50% DOPG/DOPC LUVs at various times (1, 5, and 10 min) after the addition of magainin 2. (E) Time course of magainin 2-induced leakage of calcein from a suspension of 50% DOPG/DOPC LUVs after the addition of various concentrations of magainin 2: (■) 0 μM, (□) 3 μM, (●) 4 μM, (△) 5 μM, (▲) 7 μM, and (○) 10 μM. The bars in panels A−C indicate the standard deviation.

calcein molecules among all of the examined liposomes (GUVs) at any given time, *t*, is important. Such kind of liposome was produced by the complete leakage of calcein from the liposome at any time within *t*. Thereby, we call $P_L(t)$ the fraction of completely leaked GUV at *t* or shortly the fraction of leaked GUV. Figure 3A shows the dependence of $P_L(t)$ on the magainin 2 concentration. $P_L(t)$ increased as the magainin 2 concentration increased; in the case of $t = 5$ min, at and less than 2 μM, magainin 2 did not induce the leakage [i.e., $P_L(5\text{ min}) = 0$], and $P_L(5\text{ min})$ at 3 and 4 μM were 0.10 ± 0.06 and 0.57 ± 0.11, respectively, and at ≥ 7 μM, $P_L(5\text{ min})$ was 1.0. Figure 3B shows that the fraction of intact GUV which calcein did not leak from the GUV (shortly the fraction of intact GUV) decreased with time, indicating that $P_L(t)$ increased with time. Moreover, once the leakage started, all of the fluorescent probes (i.e., calcein) were quickly lost from the GUVs (e.g., 5.6 ± 0.8 and 31.5 ± 4.7 s for 7 and 4 μM magainin 2, respectively; Figure 3C). These results indicate that the rate-determining step is the step of the pore formation, not the rate of the leakage of calcein through the pore.

We next compared the characteristics of magainin 2-induced calcein leakage from single GUVs with that from many LUVs. Figure 3E shows the time course of calcein leakage from 50% DOPG/DOPC LUVs induced by various concentrations of magainin 2. The amount of leakage from these LUVs occurred gradually over a period of 17 min, and the rate of leakage depended on the magainin 2 concentration. Figure 3D shows the dependence of the fraction of leakage of calcein from 50% DOPG/DOPC LUVs on magainin 2 concentration at 1, 5, and 10 min after mixing of the LUV suspension with the magainin 2 solution. These results resemble those obtained in the leakage experiments using the LUV suspension reported elsewhere (*7*, *8*, *10*); the leakage from many LUVs in the suspension increased gradually with time. In these leakage experiments using an ensemble of LUVs, we estimated a fraction of the leaked calcein molecules from many vesicles among all of the contents of calcein molecules in all of the vesicles. This is the average fraction of leakage from all of the vesicles, and we define it as $F_L(t)$ (%). It is related to $P_L(t)$ obtained from the single GUV experiments as follows:

$$F_L(t) = \frac{N_t P_L(t)\alpha}{N_t \alpha} \times 100 = P_L(t) \times 100 \qquad (1)$$

where α is the average number of calcein molecules in a single LUV and N_t is the number of LUVs in the suspension. Equation 1 shows that $F_L(t)$ is equal to the fraction of completely leaked LUV among all of the LUVs, $P_L(t)$. Indeed, the curve of $P_L(t)$ as a function of magainin 2 concentration (Figure 3A) is similar to that of $F_L(t)$ (Figure 3D), which supports the validity of eq 1.

Until now, it has been thought that the magainin 2-induced leakage of calcein from an ensemble of LUVs occurs

gradually from each LUV for 5−20 min; i.e., it takes a long time (5−20 min) to leak all calcein molecules from each LUV after the leakage starts (*10*). However, our results using the single GUV method indicate that the complete leakage from single GUVs occurred within less than 1 min (Figure 3C) and that $P_L(t)$ increased with time. Therefore, we can reasonably consider that the gradual increase in the leakage from an ensemble of LUVs with time (Figure 3E) is due to the increase of $P_L(t)$ and, thereby, due to an increase in the number of individual LUVs [i.e., $N_t\ P_L(t)$] that had completely lost their internal contents (i.e., calcein). The relationship between the total amount of leakage of calcein from the ensemble of LUVs [i.e., $N_t\ P_L(t)\alpha$] and the amount of calcein in a single LUV (α) is similar to that between macroscopic conductance, g, and single channel conductance, γ, of ionic channel proteins (*26*):

$$g = N_{\text{channel}} P_{\text{open}} \gamma \tag{2}$$

where N_{channel} is the number of ionic channels in the membrane and P_{open} is the probability of the open state (i.e., the fraction of open state). Most ionic channels can be in one of two states, open or closed; therefore, the open channel probability can be determined by the single channel recording. Because γ is constant, the increase in g is due to an increase in P_{open}, induced by environmental changes, such as an elevated membrane potential or increased ligand concentrations (*26*).

The small difference between the curve of P_L as a function of magainin 2 concentration (Figure 3A) and that of $F_L(t)$ (Figure 3D) was observed. For example, the magainin 2 concentration at $P_L(5\text{ min}) = 0.5$ was 3.5 μM for the single GUVs and that at $F_L(5\text{ min}) = 50\%$ was 5.8 μM for the ensemble of LUVs. For 5 μM magainin 2, the time at $P_L = 0.5$ (i.e., $t_{1/2}$) was 1.4 min for the single GUVs and that at $F_L = 50\%$ (i.e., $t_{1/2}$) was 8.0 min for the ensemble of LUVs. These data suggest apparently that magainin 2 forms the pore in the membrane more effectively in single GUVs than in the ensemble of LUVs. This phenomenon can be explained as follows. The leakage of calcein from a liposome depends on the magainin 2 concentration in the membrane interface (see The Two-State Transition Model of the Pore Formation Induced by Magainin 2 for details), which is proportional to the molar ratio of the magainin 2 bound with the membrane interface per total lipid in the solution, X_b. The value of X_b is determined by the binding constant, K, and the magainin 2 concentration immediately above the membrane interface, C_M, as follows (*27*):

$$X_b = KC_M \tag{3}$$

On the basis of Gouy−Chapman theory (*28*), C_M depends on the free (equilibrium) peptide concentration in the bulk solution, C_f, and also on the electrostatic interaction between the peptide and the membrane interface as follows (*29*):

$$C_M = C_f \exp(-ze\Psi_0/k_BT) \tag{4}$$

where z is the net electric charge of magainin 2, e the electronic charge, Ψ_0 the surface potential of the membrane, k_B the Boltzmann constant, and T the absolute temperature. The binding isotherms of magainin 2 to lipid membrane, i.e., X_b as a function of C_f, and also the binding constant, K, were determined by isothermal titration calorimetry (*27*, *29*). For example, in the binding of magainin 2 with LUVs of 1-palmitoyl-2-oleoyl-PC (POPC)/1-palmitoyl-2-oleoyl-PG (POPG) (3:1 molar ratio), X_b was 0.03 (i.e., 30 mmol/mol) at $C_f = 7$ μM in a buffer (10 mM Tris, pH 7.4, 100 mM NaCl) at 45 °C, and $K = 110\ M^{-1}$ (*27*). In the LUV suspension there is a larger area of membranes which magainin 2 binds to than in the single GUV, and thereby, the free (equilibrium) concentration of magainin 2 in the bulk solution of the LUV suspension is smaller than that in the absence of LUVs and decreases with an increase in lipid concentration as a result of the binding of magainin 2 to the membrane (*29*). As a result, the magainin 2 concentration in the membrane interface (which is proportional to X_b) decreases with an increase in lipid concentration. Therefore, the amount of leakage of calcein from the ensemble of LUVs is determined by the peptide-to-lipid molar ratio, P/L, not by the peptide concentration in the bulk solution (*10*). In our experiments of the effect of magainin 2 on the LUVs, values of P/L were in the range from 0.071 (at 3 μM magainin 2) to 0.27 (at 10 μM). On the other hand, for the single GUVs, the concentration of magainin 2 in the bulk solution is constant, the same as that of the magainin 2 solution introduced by the micropipet. Thereby, the magainin 2 concentration in the membrane interface of the GUV depends only on the magainin 2 concentration in the bulk solution, not on P/L. Applying the same method [based on the Gouy−Chapman theory (*28*)] as that used for the binding of magainin 2 to LUVs (*27*, *29*), we tried to obtain values of X_b in the interaction of various concentrations of magainin 2 with 50% DOPG/DOPC GUVs, using the same value of K as that for 25% POPG/75% POPC LUVs at 45 °C [$K = 110\ M^{-1}$ (*27*)] and the same value of z [$z = 3.8$ (*27*)]. For example, in the interaction of 7 μM magainin 2 with 50% DOPG/DOPC GUVs (Figure 1), X_b was 0.088 (i.e., 88 mmol/mol) at $C_f = 7$ μM in buffer A at 20 °C. This value may contain an error because the value of K depends on temperature, surface charge density, and curvature of the membrane. As described above, X_b (i.e., the P/L in the external monolayer of the GUVs) is an important parameter because it determines the leakage of calcein from a liposome. This estimation and the results shown in Figure 1 indicate that at a high value of X_b around 0.088 the calcein leaked quickly in all of the GUVs. On the basis of the above discussion, when we compare the results of the single GUVs and the LUV suspension (Figure 3A,D), we have to keep in mind that the free (equilibrium) magainin 2 concentration in the bulk solution for the LUV suspension is smaller than that for the single GUVs, and thereby, the magainin 2 concentration in the membrane interface of the LUV is smaller than that of the GUV. This is the main reason for the apparent result that lower concentrations of magainin 2 induced the pore formation in the membrane in single GUVs than in the ensemble of LUVs. The precise control of the peptide concentration in the bulk solution will be an advantage of the single GUV method, and thereby, we do not have to consider P/L in the single GUV method.

Shape Change of 50% DOPG/DOPC GUV Induced by Magainin 2. We performed several experiments to clarify the mechanism of the pore formation by magainin 2. Analysis of shape changes of GUVs is a highly sensitive method for detecting the interaction of substances with lipid membrane

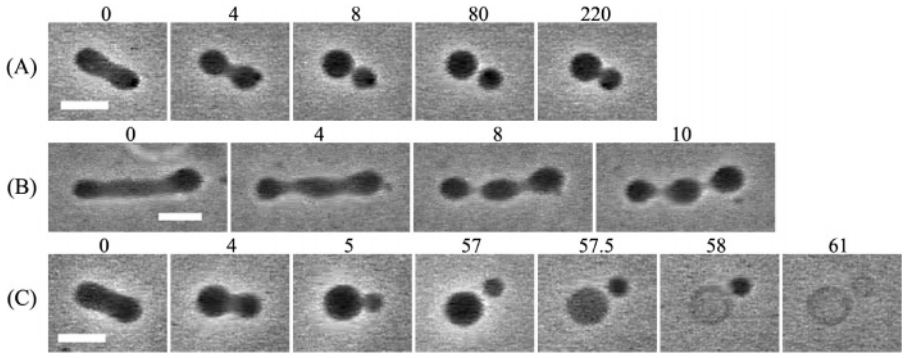

FIGURE 4: Shape changes of 50% DOPG/DOPC GUVs induced by the addition of magainin 2 at 20 °C. (A) A prolate changed into a dumbbell and then into symmetrical two spheres connected by a narrow neck upon addition of 0.5 μM magainin 2. (B) A cylinder changed into pearls on a string upon addition of 0.05 μM magainin 2. (C) A prolate changed into a pear and then into asymmetrical two spheres connected by a narrow neck upon addition of 5 μM magainin 2. The numbers above each image in panels A−C indicate the time after the addition of magainin 2. The bar corresponds to 10 μm.

(*15*, *16*). For this purpose, we use nonspherically shaped GUVs, because the shape of spherical GUVs cannot be changed without the interaction of other GUVs. Generally, when we prepare GUVs of lipid membranes in the liquid-crystalline (L_α) phase using the natural swelling method (*15*, *16*), the GUVs have many kinds of shapes such as sphere, prolate, tube, two spheres connected by a narrow neck, pearls on a string (*15*, *16*). The shape of GUVs is determined by the minimization of the elastic energy of the closed membrane, and thereby it depends on several conditions when these GUVs are formed (see below for details). In the case of GUVs of the charged lipid membrane, the spherical shape is the most dominant one, but other shapes are also formed.

To elucidate how magainin 2 interacts with the DOPG/DOPC membranes, we investigated its effect on the shapes of DOPG/DOPC GUVs. Panels A and B of Figure 4 show two kinds of shape changes in 50% DOPG/DOPC GUVs following the introduction of low concentrations (<1 μM) of magainin 2 in the vicinity of the GUV through a 20 μm diameter micropipet. In the absence of magainin 2, the GUV had a prolate shape (Figure 4A, 0 s). After the addition of 0.5 μM magainin 2, the GUV changed into a dumbbell shape (Figure 4A, 4 s) and then into two spheres connected by a neck (Figure 4A, 8 s) ($n = 8$). Further addition of magainin 2 did not change the shape (Figure 4A, 220 s). This shape change was not observed upon introduction of 0.005 μM magainin 2. Figure 4B shows another type of shape change: a cylindrical shape of GUV (Figure 4B, 0 s) changed into a series of many smaller, spherical vesicles connected by a narrow tube (so-called "pearls on a string") (Figure 4B, 10 s) ($n = 9$). Again, this shape change was not observed upon introduction of 0.005 μM magainin 2. Figure 4C shows a shape change in a 50% DOPG/DOPC GUV induced by the addition of a high concentration (5 μM) of magainin 2. A prolate (Figure 4C, 0 s) changed into two spheres connected by a neck (Figure 4C, 5 s), after which the phase contrast of the spherical vesicles was lost one by one (Figure 4C, 57.5−61 s). This indicates that magainin 2 formed a pore (or pores) in the membrane of the spherical vesicle through which sucrose and glucose could pass.

The results of Figure 4 clearly show that very low concentrations of magainin 2 induced shape changes in the 50% DOPG/DOPC GUVs. What is the mechanism for these shape changes? The shape of GUV of lipid membranes is determined by the minimization of the elastic energy of the closed membrane. It is thought that the "area-difference-elasticity" model (ADE model), also known as the "generalized bilayer-couple" model, effectively explains the shape changes of the GUV (*15*, *21*, *30*, *31*). In the ADE model, the area of each monolayer is not fixed to the equilibrium area, but the monolayer membrane can stretch elastically to increase the membrane's nonlocal elastic energy. Thus, the elastic energy of the GUV (W_{el}) can be expressed as a sum of the membrane bending energy and the energy of the relative monolayer stretching. In the ADE model, the shape of the GUV is determined by the minimization of the membrane elastic energy (W_{el}) for a given area A, volume V, and difference [$\Delta A_0 (= A_0^{ex} - A_0^{in})$] between the area of the external (A_0^{ex}) and internal monolayers (A_0^{in}) in the GUV bilayer membrane under the relaxed (i.e., nonstretched) condition (*30*, *31*). The analysis based on the ADE model shows that, under the condition of the constant volume of the GUV, the shape changes as follows: as ΔA_0 increases, (1) a prolate → a pear (i.e., asymmetric prolate) or a dumbbell (i.e., symmetric prolate) → two spheres connected by a narrow neck and (2) a cylinder → pearls on a string. These shape changes are the same as those induced by magainin 2 in the 50% DOPG/DOPC GUVs (Figure 4). This analysis therefore shows that magainin 2 binds to the membrane interface of the external monolayer of the GUVs from the outside aqueous solution, increasing the ΔA_0 of the GUVs. At the first step of the binding, magainin 2 binds to the surface of the membrane interface as a result of the electrostatic attraction between the positive charges of magainin 2 and the negative charge of DOPG in the membrane interface. This may decrease the area of the external monolayer as a result of the neutralization of the charges on the DOPG molecules. Magainin 2 can then be partitioned deeply into the membrane interface owing to its high interfacial hydrophobicity (*16*, *22*, *32*), inducing an increase in the steric repulsion between the peptide and the hydrophilic segments of lipids in the membrane interface, which increases the area of the external monolayer. In our previous report, we clearly showed that a de novo designed peptide (WLFLLKKK) containing a segment with high interfacial hydrophobicity (WLFLL) can bind to the electrically neutral membrane interface of a DOPC membrane, increasing the area of the monolayer membrane (*16*). Magainin 2 has many Phe and Leu residues, which have high

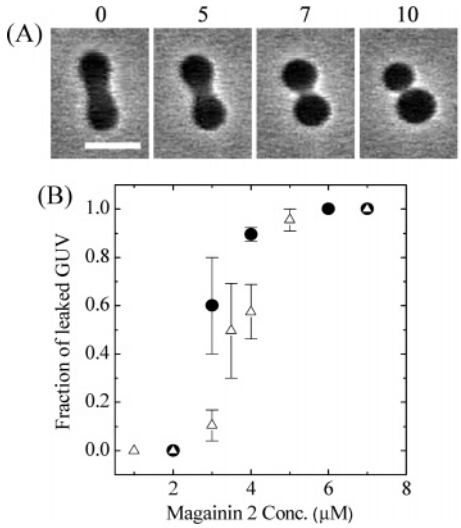

FIGURE 5: (A) Shape change of a 50% DOPG/DOPC GUV induced by the addition of 5 μM lyso-PC at 20 °C. A prolate changed into symmetrical two spheres connected by a narrow neck. The bar corresponds to 10 μm. (B) Effect of lyso-PC in the external monolayer on the dose−response of magainin 2 on the fraction of completely leaked GUV, P_L(5 min), in the presence (●) and absence (△) of 5 μM lyso-PC. The bar indicates the standard deviation.

interfacial hydrophobicity; therefore, after neutralization of positive charges of Lys residues, the peptide has a high interfacial hydrophobicity so that it can partition deeply in the membrane interface. This effect on the area of the external monolayer is greater than that of the electric neutralization. Thus, the main reason for changes in the shape of the GUVs is that magainin 2 increases the membrane area of the external monolayer of the GUVs by binding to the membrane interface.

Effect of Lysophosphatidylcholine (Lyso-PC) on the Magainin 2-Induced Leakage of Calcein from DOPG/DOPC GUVs. We investigated the effect of the surface pressure in the external monolayer of GUVs on the pore formation. To increase the surface pressure, we solubilized 5 μM lyso-PC (16:0), which is less than the critical micelle concentration, in the solution outside the GUVs before the addition of magainin 2. Generally, lyso-PC in the external solution enters into the external monolayer membrane of GUVs, which increases the area of the monolayer and its surface pressure (*21*). In the case of 50% DOPG/DOPC GUVs, 5 μM lyso-PC (16:0) induced a shape change such as the prolate to two spheres connected by a neck (Figure 5A) ($n = 12$), indicating that the lyso-PC in the external solution enters into the external monolayer of 50% DOPG/DOPC GUVs, which increases the area of the monolayer and its surface pressure. Figure 5B shows the dependence of P_L(5 min) on the magainin 2 concentration in the presence and absence of 5 μM lyso-PC. At all concentrations of magainin 2, the $P_L(t)$ values were higher in the presence than in the absence of lyso-PC, suggesting that the increase in the surface pressure in the external monolayer increases the rate of the pore formation.

The Two-State Transition Model of the Pore Formation Induced by Magainin 2. We propose a hypothesis of the two-state transition model to describe the pore formation by magainin 2 in the membrane. The first state (B_{ex} state) is the binding state of magainin 2 to the external monolayer membrane of the liposomes, where magainin 2 forms the α-helix parallel to the membrane surface (*5*, *6*), and the second state (P state) is the pore state in the membrane. As a model of the structure of the pore in the membrane formed by magainin 2, the toroidal (wormhole) pore is generally considered (*9*, *33*). In this model, the membrane surface bends in a toroidal fashion to create a pore. At present, we do not know the number of the pores in the membrane formed by magainin 2 in the P state. The rate constant of the transition from the B_{ex} state to the P state, k_P, depends on activation energy (energy barrier), E_P, and is given by the equation:

$$k_P = A \exp(-E_P/k_B T) \quad (5)$$

where k_B is the Boltzmann constant and T is the absolute temperature. However, individual events of the two-state transition occur stochastically, which has been well demonstrated by the transition between open and closed states of single ionic channels (*34*) and by the force-induced unfolding of proteins (*35*). To estimate the rate constant k_P, we have to obtain the fraction of the B_{ex} state of GUVs among all of the examined GUVs. If we assume that the pore formation occurred by the irreversible two-state transition from the B_{ex} state to the P state, the fraction of the B_{ex} state can be determined by the fraction of intact GUV which calcein did not leak (shortly the fraction of intact GUV), $P_{intact}(t)$. Experimentally, we obtained the time at which the rapid decrease in the fluorescence intensity of a GUV started (Figures 1C and 2C), and we define the state of GUV before this time as the B_{ex} state. On the other hand, the P state can be defined as the state of GUV which calcein is leaking or the state of GUV which calcein was completely leaked (i.e., did not contain any calcein molecules), and thereby, the fraction of the P state can be expressed as $1 - P_{intact}(t)$. Figure 3B shows the time course of the fraction of the B_{ex} state (i.e., the fraction of intact GUV) in the presence of various concentrations of magainin 2. The fraction of the B_{ex} state can be expressed using the rate constant, k_P, as follows:

$$P_{intact}(t) = \exp[-k_P(t - t_{eq})] \quad (6)$$

where t_{eq} is an adjustable parameter. At present, we do not know the exact time required for the equilibration of the magainin 2 concentration in the vicinity of a GUV and the time required for the binding equilibrium of magainin 2 from aqueous solution to the membrane interface of the GUV. We can reasonably consider that t_{eq} is the time when the binding equilibrium of magainin 2 is attained, and thereby the state of the GUV becomes the B_{ex} state at t_{eq}. As shown in Figure 3B, all of the curves of the time course of the fraction of the B_{ex} state were well fitted by a single exponential function defined by eq 6. Table 1 shows values

Table 1: Rate Constant from the B_{ex} State to the P State and Time Required for the Binding Equilibrium of Magainin 2 in the Presence of Various Concentrations of Magainin 2

magainin 2 conc (μM)	rate constant from B_{ex} state to P state, k_P (min^{-1})	time required for binding equilibrium of magainin 2, t_{eq} (s)
10	1.6	2
7	1.1	7
5	0.76	10
4	0.18	23

of two parameters, k_P and t_{eq}. The rate constant increased with an increase in magainin 2 concentration, and k_P for 10 μM magainin 2 (1.6 min^{-1}) was about 10 times larger than k_P of 4 μM magainin 2 (0.18 min^{-1}). Values of t_{eq} were less than 30 s and decreased a little with an increase in magainin 2 concentration. We can consider that the rate of the binding equilibrium is larger at higher concentration of magainin 2 in the solution. This may explain the dependence of t_{eq} on the magainin 2 concentration. These results suggest that the pore formation induced by magainin 2 occurs by the two-state transition.

From the data in this report, we cannot determine the mechanism of the two-state transition clearly. However, we propose a hypothesis of the mechanism for future investigation as follows. Figures 3A and 4A,B show that the shape changes in the GUVs were induced at very low concentrations of magainin 2, which could not induce the pore formation in the membrane. Figure 4C indicates that at high concentration of magainin 2 the shape change in the GUV occurred prior to the pore formation. The kind of these shape changes indicates that the area of the external monolayer of the GUV increases with an increase in the amount of the magainin 2 bound to the external monolayer of the GUV. This raises the surface pressure of the external monolayer and increases the stretching of the internal monolayer of the GUV, destabilizing the B_{ex} state (*21*). Hence, as the amount of the bound magainin 2 in the external monolayer increases, the free energy of the B_{ex} state increases, causing a decrease in the activation energy E_p. As a result, the rate constant of the transition from the B_{ex} state to the P state increases as the magainin 2 concentration is raised. This hypothesis of the mechanism is consistent with several results, such as the dependence of P_L on the magainin 2 concentration (Figure 3A) and the effect of lyso-PC on P_L (Figure 5B). In addition, lyso-PC and magainin 2 are also known as the substance to favor the positive curvature of the membrane (*10*), and thereby, these substances may decrease the free energy of the transition state from the B_{ex} state to the P state and, thereby, decrease the activation energy. At present, we do not know which effect of magainin 2 and lyso-PC is dominant. As a result of the large structural changes involved in the transition from the B_{ex} state to the P state, as well as the prior destabilization of the internal monolayer (due to the large stretching), some magainin 2 molecules and some lipids in the external monolayer may reach the internal monolayer of liposomes. This can reasonably explain the observed flip-flop of lipids and magainin 2 from the external to the internal monolayer (*7*, *33*).

In the P state, the fluorescence intensity of the GUV, $I(t)$, decayed almost exponentially with time. Figure 1B shows that the time course of the rapid decrease in the fluorescence intensity of the GUV in the presence of 7 μM magainin 2 was well fitted by a curve represented by the equation:

$$I(t) = I(t_{tr}) \exp[-k_{leak}(t - t_{tr})] \quad (7)$$

where t_{tr} is the time when the rapid decrease in the fluorescence intensity began to occur, $I(t_{tr})$ is the fluorescence intensity at t_{tr}, and k_{leak} is the decay constant of the fluorescence intensity. Here we used an approximation that the amount of the photobleaching during the leakage of calcein was negligible for simplicity. The average value of k_{leak} for 7 μM magainin 2 [i.e., $k_{leak}(7\ \mu M)$] was 0.46 ± 0.06 s^{-1}. Similarly, in the case of 4 μM magainin 2, the rapid decrease in the fluorescence intensity was also well fitted by a curve represented by eq 7 (Figure 2B). The average value of k_{leak} for 4 μM magainin 2 [$k_{leak}(4\ \mu M)$] was 0.09 ± 0.04 s^{-1}, which is smaller than k_{leak} (7 μM). If we assume that the lifetime of the P state is longer than the duration which the rapid decrease in the fluorescence intensity occurred (i.e., 5.6 ± 0.8 and 31.5 ± 4.7 s for 7 and 4 μM magainin 2, respectively), the decrease in the fluorescence intensity is due to the leakage of calcein through the pores which were formed at the two-state transition from the B_{ex} state to the P state. We can roughly estimate the membrane permeability of calcein through the pore as follows. The fluorescent probe, calcein, diffuses through the pore from the inside to the outside of the GUV. Generally, the membrane permeability can be expressed by the flux of a substance, J, per unit area of membrane [mol/(cm^2·s)], which is derived by Fick's law (*36*):

$$J = -P[C^{in}(t) - C^{out}(t)] \quad (8)$$

where P is permeability coefficient of the substance in the membrane and $C^{in}(t)$ and $C^{out}(t)$ are the concentration of the substance inside of a GUV and that outside of the GUV at time t, respectively. Thereby, the rate of leakage of calcein from a GUV can be expressed as follows (here we assume $C^{out} = 0$ for any time, because the volume of the outside of the GUV is very large):

$$dC^{in}/dt = -4\pi r^2 P C^{in}$$

$$\therefore C^{in}(t) = C_0^{in} \exp(-4\pi r^2 P t) \quad (9)$$

where r is the radius of the GUV and C_0^{in} is the concentration of calcein inside the GUV before the leakage. It is reasonable to consider that the concentration of calcein inside the GUV is roughly proportional to the fluorescence intensity of the GUV. From a comparison of eq 7 with eq 9, we can conclude that $P \propto k_{leak}$. Using this relationship, we can determine the ratio of P for 7 μM magainin [P(7 μM)] to P for 4 μM magainin [P(4 μM)] as follows:

$$\frac{P(7\ \mu M)}{P(4\ \mu M)} = \frac{k_{leak}(7\ \mu M)}{k_{leak}(4\ \mu M)} = \frac{0.46}{0.09} = 5 \quad (10)$$

The membrane permeation of calcein characterized by the permeability coefficient, P, is determined by the pore formed by magainin 2 in the membrane. If the size of the pore of magainin 2 does not depend on the magainin 2 concentration, eq 10 indicates that the number density of the pore in the membrane at 7 μM magainin 2 is 5 times higher than that at 4 μM magainin 2. If not, eq 10 indicates that the size of the pore at 7 μM magainin 2 is larger than that at 4 μM magainin 2.

We do not currently know the lifetime of the pore formed by magainin 2 in the membrane. We expect that, eventually, another two-state transition occurs from the P state to the binding state of magainin 2 in the internal monolayer membrane of the liposomes (the B_{in} state). Matsuzaki and colleagues considered that the pore state is the transition state of the translocation of magainin 2 from the B_{out} state to the

B_{in} state, and thereby, the lifetime of the pore is very small (*7*, *10*). On the other hand, Huang and colleagues suggested that the pore state is very stable at high P/L (>1/30), and thereby, they succeeded in the crystallization of the pores formed by magainin 2 in the membrane (*9*, *37*). We can roughly estimate the value of P/L of the interaction of magainin 2 with a GUV. As a typical situation in our experiment, there is one GUV with a radius of 10 μm in a cubic region of an aqueous solution (side 100 μm). If we assume the average area of phospholipids in the membrane of a GUV is 70 Å^2 [the molecular area of DOPC is 72.5 Å^2 (*38*)], we obtain that the lipid concentration in this cubic region is 6.0 μM. When the magainin 2 concentration is in the range from 3.0 to 10 μM, the value of P/L is in the range from 0.5 to 1.7, which is larger than 1/30. Thereby, we can consider that, under this condition, the pore state is stable. Therefore, at present, we consider that our data obtained using the single GUV method suggest the longer lifetime of the P state of magainin 2 than the duration of the leakage of calcein. However, we do not have any experimental evidence for the lifetime of the P state. We are now developing a new method to estimate the lifetime of the P state using the single GUV method. If the lifetime of the P state is shorter than 1 s, this suggests that multiple pores are produced one by one during the leakage process. This may be possible because the membrane is so destabilized due to a large structural change of the membrane at the transition from the P state to the B_{in} state that the activation energy, E_P, may decrease greatly, increasing the rate of transition from the B_{ex} to the P state, k_P, greatly. Additional data and analysis are needed to determine which of these possibilities is correct.

CONCLUSION

Our investigation of the interaction of magainin 2 with lipid membranes using the single GUV method directly shows that magainin 2 forms the pore in the membrane. The rapid leakage of the fluorescent probe (calcein) from a GUV started stochastically, and once it began, the complete leakage occurred rapidly within about 1 min. This result indicates that the pore formation is the rate-determining step, not the leakage rate. In contrast, the leakage from a suspension of many LUVs occurred gradually over a 10−20 min period. Thereby, the fraction of completely leaked liposome at a specific time, $P_L(t)$, is an important parameter to understand the mechanism of the magainin 2-induced leakage. Experimental results show that $P_L(t)$ increased with time. Therefore, we can reasonably consider that the gradual increase in the leakage from many LUVs with time is due to the increase in $P_L(t)$. Furthermore, as the magainin 2 concentration increased, $P_L(t)$ increased. On the basis of our results, we proposed the two-state transition model for the magainin 2-induced pore formation. The rate constant of the transition from the B_{ex} state to the P state was estimated, and it increased with an increase in magainin 2 concentration. In summary, using the single GUV method we succeeded in obtaining new information on the magainin 2-induced pore formation in the membrane. For further analysis, we have to improve the experimental methods and data analysis of the single GUV method. Our results in this report and the result of Ambroggio et al. (*25*) indicate that the GUV is a promising tool for the investigation on the interaction of the antibiotic peptides with lipid membranes. We believe that the single GUV method (including the analysis method of the data) described here will provide a great deal of new information on the mechanism of antibiotic peptides and substances with antibiotic activity.

ACKNOWLEDGMENT

We thank Mr. Yasuyuki Inaoka for helpful discussions.

REFERENCES

1. Zasloff, M. (2002) Antimicrobial peptides of multicellular organisms, *Nature 415*, 389−395.
2. Hwang, P. M., and Vogel, H. J. (1998) Structure−function relationships of antimicrobial peptides, *Biochem. Cell Biol. 76*, 235−236.
3. Zasloff, M. (1987) Magainins, a class of antimicrobial peptides from *Xenopus* skin: Isolation, characterization of two active forms, and partial cDNA sequence of a precursor, *Proc. Natl. Acad. Sci. U.S.A. 84*, 5449−5453.
4. Zasloff, M., Martin, B., and Chen, H.-C. (1988) Antimicrobial activity of synthetic magainin peptides and several analogues, *Proc. Natl. Acad. Sci. U.S.A. 85*, 910−913.
5. Bechinger, B., Zasloff, M., and Opella, S. J. (1993) Structure and orientation of the antibiotic peptide magainin in membranes by solid-state nuclear magnetic resonance spectroscopy, *Protein Sci. 2*, 2077−2084.
6. Hirsh, D. J., Hammer, J., Maloy, W. L., Blazyk, J., and Schaefer, J. (1996) Secondary structure and location of a magainin analogue in synthetic phospholipid bilayers, *Biochemistry 35*, 12733−12741.
7. Matsuzaki, K., Murase, O., Fujii, N., and Miyajima, K. (1995) Translocation of a channel-forming antimicrobial peptide, magainin 2, across lipid bilayers by forming a pore, *Biochemistry 34*, 6521−6526.
8. Boggs, J. M., Jo, E., Polozov, I. V., Epand, R. F., Anantharamaiah, G. M., Blazyk, J., and Epand, R. M. (2001) Effect of magainin, class L, and class A amphipathic peptides on fatty acid spin labels in lipid bilayers, *Biochim. Biophys. Acta 1511*, 28−41.
9. Ludtke, S. J., He, K., Heller, W. T., Harroun, T. A., Yang, L., and Huang, H. W. (1996) Membrane pores induced by magainin, *Biochemistry 35*, 13723−13728.
10. Matsuzaki, K., Sugishita, K., Ishibe, N., Ueha, M., Nakata, S., Miyajima, K., and Epand, R. M. (1998) Relationship of membrane curvature to the formation of pores by magainin 2, *Biochemistry 37*, 11856−11863.
11. Evans, E., and Rawicz, W. (1990) Entropy-driven tension and bending elasticity in condensed-fluid membranes, *Phys. Rev. Lett. 64*, 2094−2097.
12. Farge, E., and Devaux, P. F. (1992) Shape changes of giant liposomes induced by an asymmetric transmembrane distribution of phospholipids, *Biophys. J. 61*, 347−357.
13. Saitoh, A., Takiguchi, K., Tanaka, Y., and Hotani, H. (1998) Opening-up of liposomal membranes by talin, *Proc. Natl. Acad. Sci. U.S.A. 95*, 1026−1031.
14. Tsumoto, K., Nomura, S., Nakatani, Y., and Yoshikawa, K. (2001) Giant liposome as a biochemical reactor: transcription of DNA and transportation by laser tweezers, *Langmuir 17*, 7225−7228.
15. Tanaka, T., Tamba, Y., Masum, S. M., Yamashita, Y., and Yamazaki, M. (2002) La^{3+} and Gd^{3+} induce shape change of giant unilamellar vesicles of phosphatidylcholine, *Biochim. Biophys. Acta 1564*, 173−182.
16. Yamashita, Y., Masum, S. M., Tanaka, T., and Yamazaki, M. (2002) Shape changes of giant unilamellar vesicles of phosphatidylcholine induced by a de novo designed peptide interacting with their membrane interface, *Langmuir 18*, 9638−9641.
17. Yamazaki, M., Ohnishi, S., and Ito, T. (1989) Osmoelastic coupling in biological structures: decrease in membrane fluidity and osmophobic association of phospholipid vesicles in response to osmotic stress, *Biochemistry 28*, 3710−3715.
18. Yamazaki, M., and Ito, T. (1990) Deformation and instability in membrane structure of phospholipid vesicles caused by osmophobic association: mechanical stress model for the mechanism of poly(ethylene glycol)-induced membrane fusion, *Biochemistry 29*, 1309−1314.
19. Yamazaki, M., and Tamba, Y. (2005) The single GUV method for probing biomembrane structure and function, *e−J. Surf. Sci. Nanotechnol. 3*, 218−227.

20. Tanaka, T., and Yamazaki, M. (2004) Membrane fusion of giant unilamellar vesicles of neutral phospholipid membranes induced by La^{3+}, *Langmuir 20*, 5160−5164.
21. Tanaka, T., Sano, R., Yamashita, Y., and Yamazaki, M. (2004) Shape changes and vesicle fission of giant unilamellar vesicles of liquid-ordered phase membrane induced by lysophosphatidylcholine, *Langmuir 20*, 9526−9534.
22. Masum, S. M., Li, S. J., Tamba, Y., Yamashita, Y., Tanaka, T., and Yamazaki, M. (2003) Effect of de novo designed peptides interacting with the lipid-membrane interface on the stability of the cubic phases of the monoolein membrane, *Langmuir 19*, 4745−4753.
23. Tamba, Y., Tanaka, T., Yahagi, T., Yamashita, Y., and Yamazaki, M. (2004) Stability of giant unilamellar vesicles and large unilamellar vesicles of liquid-ordered phase membranes in the presence of Triton X-100, *Biochim. Biophys. Acta 1667*, 1−6.
24. Ambroggio, E. E., Kim, D. H., Separovic, F., Barrow, C. J., Barnham, K. J., Bagatolli, L. A., and Fidelio, G. D. (2005) Surface behavior and lipid interaction of Alzheimer β-amyloid peptide 1−42: a membrane-disrupting peptide, *Biophys. J. 88*, 2706−2713.
25. Ambroggio, E. E., Separovic, F., Bowie, J. H., Fidelio, G. D., and Bagatolli, L. A. (2005) Direct visualization of membrane leakage induced by the antibiotic peptides: maculatin, citropin, and aurein, *Biophys. J. 89*, 1874−1881.
26. Hille, B. (1992) *Ionic Channels of Excitable Membranes*, 2nd ed., Sinauer Associates, Sunderland, MA.
27. Wieprecht, T., Apostolov, O., and Seelig, J. (2000) Binding of the antibacterial peptide magainin 2 amide to small and large unilamellar vesicles, *Biophys. Chem. 85*, 187−198.
28. McLaughlin, S. (1989) The electrostatic properties of membranes, *Annu. Rev. Biophys. Biophys. Chem. 18*, 113−136.
29. Wenk, M. R., and Seelig, J. (1998) Magainin 2 amide interaction with lipid membranes: calorimetric detection of peptide binding and pore formation, *Biochemistry 37*, 3909−3916.
30. Heinrich, V., Svetina, S., and Zeks, B. (1993) Nonaxisymmetric vesicle shapes in a generalized bilayer-couple model and the transition between oblate and prolate axisymmetric shapes, *Phys. Rev. E: Stat., Nonlinear, Soft Matter Phys. 48*, 3112−3123.
31. Miao, L., Seifert, U., Wortis, M., and Döbereiner, H.-G. (1994) Budding transitions of fluid-bilayer vesicles: The effect of area-difference elasticity, *Phys. Rev. E: Stat., Nonlinear, Soft Matter Phys. 49*, 5389−5407.
32. Wimley, W. C., and White, S. H. (1996) Experimentally determined hydrophobicity scale for proteins at membrane interface, *Nat. Struct. Biol. 3*, 842−848.
33. Matsuzaki, K., Murase, O., Fujii, N., and Miyajima, K. (1996) An antimicrobial peptide, magainin 2, induced rapid flip-flop of phospholipids coupled with pore formation and peptide translocation, *Biochemistry 35*, 11361−11368.
34. Sakmann, B., and Neher, E., Eds. (1983) *Single-Channel Recording*, Plenum Press, New York.
35. Rief, M., Fernandez, J. M., and Gaub, H. E. (1998) Elastically coupled two-level systems as a model for biopolymer extensibility, *Phys. Rev. Lett. 81*, 4764−4768.
36. Schultz, S. G. (1980) *Basic Principles of Membrane Transport*, Cambridge University Press, Cambridge, U.K.
37. Yang, L., Weiss, T. M., Lehrer, R. I., and Huang, H. W. (2000) Crystallization of antimicrobial pores in membranes: magainin and protegrin, *Biophys. J. 79*, 2002−2009.
38. Nagle, J. F., and Tristram-Nagle, S. (2000) Structure of lipid bilayers, *Biochim. Biophys. Acta 1469*, 159−195.

BI051684W